

Interval-Based Identification of Friction and Hysteresis Models*

Andreas Rauh, Julia Kersten, and Harald Aschemann
University of Rostock, Chair of Mechatronics,
Justus-von-Liebig-Weg 6, D-18059 Rostock, Germany
{Andreas.Rauh, Julia.Kersten, Harald.Aschemann}@uni-rostock.de

Abstract

Reliable parameter identification for dynamic systems has to take into account mathematical models that are predefined by domain-specific modeling assumptions. For example, these assumptions result from the basic physical principles for the derivation of the equations of motion for mechanical multibody systems or from the fundamental laws describing electric circuits. During the identification, it is essential to determine those parameter ranges that are simultaneously consistent with the before-mentioned model structures and the measured data. Typically, measured data are corrupted by random noise with certain probability density functions and (bounded) errors due to limited sensor resolution. In this paper, it is assumed that disturbances, summarizing all non-modeled external influences acting onto the sensor signals, are described by worst-case interval bounds. Then, the task of parameter identification results in the (recursive) computation of closed intervals for all unknown parameters. Moreover, parameters that may change their values depending on current operating conditions have to be treated suitably by the identification procedure. To make the parameter identification as efficient as possible, an approach for the sensitivity-based input optimization is presented which aims (i) at reducing possible ambiguities between various parameters and (ii) at the speed-up of the identification so that the required experiments can be made as short as possible. The before-mentioned strategies for avoiding ambiguities are especially necessary if a class of hybrid systems is considered. These hybrid systems are characterized by state- and input-dependent transitions between different continuous-time state-space representations.

Keywords: Interval-based parameter identification, Friction, Hysteresis, Verified solution of non-smooth ordinary differential equations

AMS subject classifications: 65G30,65G40,34A38,93B30

*Submitted: December 20, 2016; Revised: July 3, 2017; Accepted: August 25, 2017.

1 Introduction

Dynamic system models with state- and input-dependent transitions between different continuous-time state-space representations are common for the mathematical modeling of a large variety of technical systems. Among these, especially the description of friction and hysteresis by piecewise defined analytic expressions is widely used in both mechanical engineering and control engineering [3, 14, 15, 16]. The same holds for hysteresis effects that are ubiquitous in electro-magnetic circuits.

In previous work, interval-based simulation algorithms were developed for the computation of guaranteed state enclosures for initial value problems (IVPs) of ordinary differential equations (ODEs) with piecewise-defined right-hand sides [1, 9, 12, 17, 18]. These simulations were then included in parameter identification routines, in which the computed state enclosures are compared with measured data for selected state variables with bounded errors. Hence, the verified simulation of these ODEs with non-smooth right-hand sides is the basic building block for a model-based recursive parameter identification. The corresponding identification algorithms are implemented in a predictor-corrector framework, where the verified simulation is employed between two subsequent points of time at which measurements become available. The consistency of the simulated state enclosures on the one hand and the measured data on the other hand is then ensured by suitable interval Newton methods [5, 10], contractor techniques [4], or (in the simplest possible situation) by directly intersecting the simulated and measured intervals¹.

As a benchmark application, the experimental identification of the mathematical model of a drive train test rig is considered in this paper. The corresponding set of ODEs with non-smooth right-hand sides is given in terms of an automaton representation for all possible transitions between static friction and a piecewise linear, velocity-proportional model for sliding friction. Coefficients for the rotary mass moment of inertia, the velocity-proportional sliding friction, and the initial breakaway torque have to be identified experimentally by using only angle measurements determined by an encoder with a finite resolution. The corresponding measurement errors can therefore be described in terms of an additive interval variable [14, 15].

To make the fundamental identification procedure applicable for further — especially more complex — system models, algorithmic extensions are developed which allow for preventing an excessive growth of the computational effort if a larger number of uncertain parameters are considered. On the one hand, this involves the derivation of problem-specific subdivision routines for the exclusion of those parameter ranges that are definitely inconsistent² with the measured data and the given system model. On the other hand, these subdivision heuristics tend to become excessively complex for systems with a large number of unknown parameters. Therefore, it is necessary to derive optimal inputs allowing for the excitation of the system in such a way that the required parameter values can be estimated in an optimal way with respect to a certain performance criterion. These procedures make use of the differential sensitivities

¹Besides the contraction of the predicted, i.e., simulated state intervals, these techniques also allow for fault detection or for a falsification of modeling assumptions in cases in which state intervals that are compatible with the measured data do not intersect with the predicted enclosures of the state trajectories.

²Throughout this paper, *consistent parameter intervals* are those parameter ranges that lead to predicted states of the system ODEs that can be explained by the available measurements, while *inconsistent parameter intervals* are characterized by empty intersections of the measured values and the corresponding simulated quantities.

of state trajectories in operating regimes where the dynamics can be described locally by means of an ODE with a smooth right-hand side.

This paper is structured as follows. Starting with the description of a motivating benchmark scenario (Sec. 2), that is used for the experimental parameter identification of a drive train test rig at the Chair of Mechatronics at the University of Rostock, simulation routines for ODEs with non-smooth right-hand sides and recursive parameter identification procedures are reviewed in Secs. 3 and 4. The optimal input design in Sec. 5 aims at the fastest possible parameter identification with reduced ambiguities between the individual piecewise smooth system models of a hybrid dynamic system given in the before-mentioned automaton representation. Experimental results for the parameter identification are summarized in Sec. 6 before the paper is concluded in Sec. 7 with an outlook on future work.

2 Benchmark Application

Figs. 1 and 2 give an overview of the drive train test rig that is used as an experimental benchmark application for the verified parameter identification scheme considered in this paper [14, 15]. It consists of an electric drive (operated in torque controlled mode) that is rigidly attached to the drive-side shaft. Both shafts in Fig. 1 are connected to each other via a toothed belt. This belt can be assumed to have negligible elasticity, so that the major dynamics result from the acceleration and deceleration of the overall mass moment of inertia (β^{-1}) and from velocity-proportional friction (due to actuation of a magnetic powder brake on the load-side shaft, characterized by the parameter α). Static friction, which may change its value after each standstill is given by the value $T_{F,s}$.

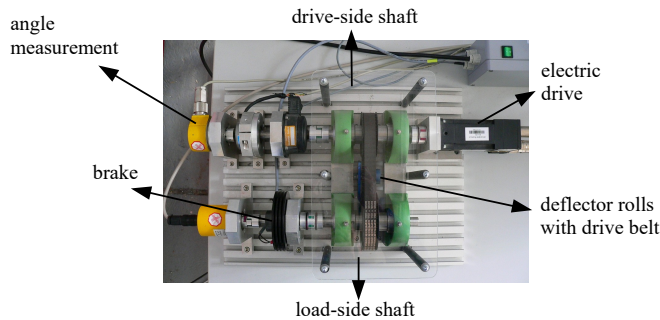


Figure 1: Test rig for the experimental parameter identification.

According to [14, 15], the state equations of the drive train test rig are given by

$$\begin{bmatrix} \dot{x}_1(t) \\ \dot{x}_2(t) \end{bmatrix} = \begin{bmatrix} x_2(t) \\ \alpha \cdot x_2(t) + \beta \cdot (u(t) - T_F(t)) \end{bmatrix} \quad (1)$$

with the breakaway torque

$$T_F(t) = T_{F,s} \cdot \text{sign}(x_2(t)) \quad . \quad (2)$$

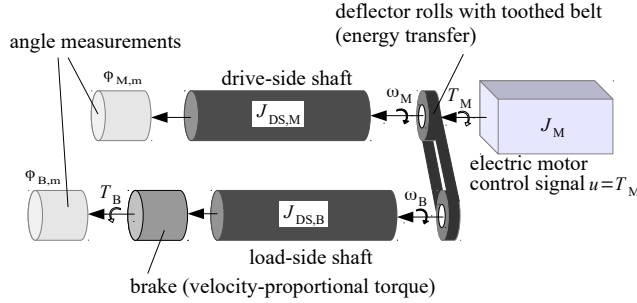


Figure 2: Modeling of the test rig: Definition of system components and relevant variables.

For the case of standstill, the state equations turn into

$$\begin{bmatrix} \dot{x}_1(t) \\ \dot{x}_2(t) \end{bmatrix} = \begin{bmatrix} 0 \\ 0 \end{bmatrix}. \quad (3)$$

The state transition diagram in Fig. 3 summarizes all possible events in which transitions between the discrete models S_1 for sliding friction with negative angular velocities $\omega_M = x_2 < 0$, S_3 for sliding friction with positive angular velocities $x_2 > 0$, and for standstill (S_2 with $x_2 = 0$) become active³.

Although the individual discrete submodels S_i , $i \in \{1, 2, 3\}$, are mutually exclusive in the case of a simulation with exactly known parameters, the interval-based simulation routine presented in the following section with uncertain parameters $\alpha \in [\alpha]$, $\beta \in [\beta]$, and $[T_{F,s}] := [\underline{T}_{F,s}; \overline{T}_{F,s}]$ has to be capable of tracing scenarios in which also more than one of the submodels S_i may be active at a time (cf. Fig. 4). These situations arise, for example, if the simulated velocity intervals $[x_2]$ simultaneously contain the value zero as well as positive and/or negative values.

Note that for the uncertain model in Fig. 4, the following definitions hold for the system input $\tilde{u}(t) := u(t) - T_F(t)$ and for the worst-case influence of static friction $[T_F^{\max}] := [-\overline{T}_{F,s}; \overline{T}_{F,s}]$.

After an overview of the underlying simulation procedure for the uncertain ODE system with a non-smooth right-hand side, the static and sliding friction parameters as well as the mass moment of inertia are identified with an interval implementation of an observer-based predictor-corrector identification procedure.

3 Interval-Based Verified Simulation Procedure

Because measured data are only available at equidistant temporal sampling points for the identification of system parameters, a verified simulation routine is employed in the prediction stage of the observer-based approach presented in the following section that is based on a discretization of the considered time horizon.

³Note that the modes S_1 and S_3 differ in the sign of the breakaway torque in (2).

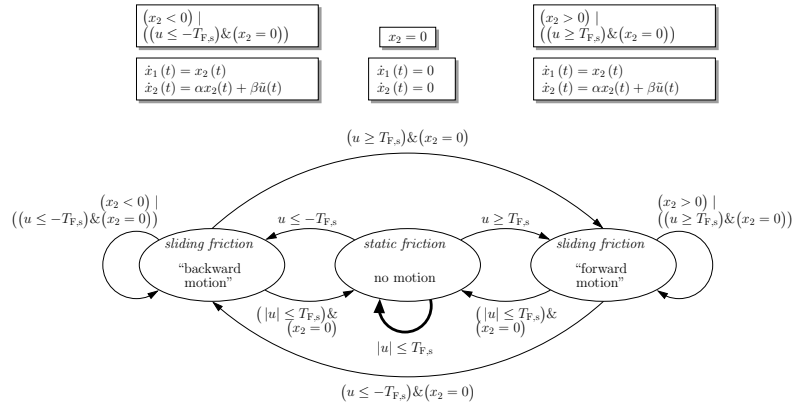


Figure 3: State transition diagram (automaton representation) for switchings between sliding and static friction modes with nominal parameters (all discrete model states are mutually exclusive).

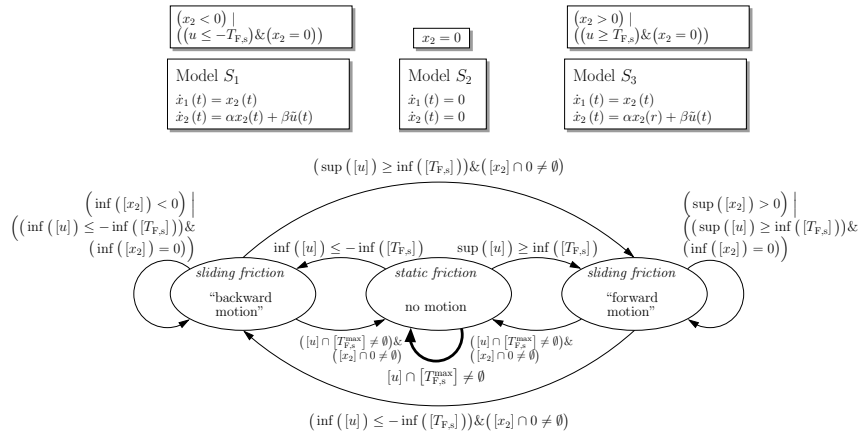


Figure 4: State transition diagram for switchings between sliding and static friction modes with uncertain parameters.

According to

$$\mathbf{x}(t_{k+1}) = \mathbf{x}(t_k) + \sum_{i=1}^{\nu} \frac{h^i}{i!} \mathbf{f}^{(i-1)}(\mathbf{x}(t_k), \mathbf{p}, \mathbf{u}(t_k), t_k) + \mathbf{e}(\mathbf{x}(\xi), \mathbf{p}, \mathbf{u}(\xi), \xi), \quad (4)$$

$$\dot{\mathbf{x}}(t_k) := \mathbf{f}(\mathbf{x}(t_k), \mathbf{p}, \mathbf{u}(t_k), t_k), \quad \mathbf{x}(t_k) \in \mathbb{R}^n, \quad \mathbf{p} \in \mathbb{R}^{n_p},$$

a Taylor series expansion (c.f [6, 8] for further details) of the solution of the IVP with respect to time is performed with the integration step-size h , i.e., $t_k = kh$, $t_{k+1} = (k+1)h$, and $t_k \leq \xi \leq t_{k+1}$.

For the implementation of the verified simulation routine, the following assumptions are made⁴:

- All system parameters $\mathbf{p} \in [\mathbf{p}]$ are piecewise constant between two subsequent sampling points t_k and t_{k+1} .
- Changes of the control signals $\mathbf{u}(t_k)$ only occur at the discretization points $t = t_k$.
- A recursive computation of the total derivatives $\mathbf{f}^{(i-1)}$ (resp. of the Taylor series coefficients of the state trajectories) is performed in terms of *smooth* right-hand sides $\mathbf{f} \in C^\nu$ of the ODE with $\dot{\mathbf{p}} = \mathbf{0}$ and $\dot{\mathbf{u}}(t) = \mathbf{0}$ for each open time interval $t_k < t < t_{k+1}$.
- Guaranteed bounds of the discretization error are computed by

$$\mathbf{e}(\mathbf{x}(\xi), \mathbf{p}, \mathbf{u}(\xi), \xi) \subseteq [\mathbf{e}_k] := \frac{h^{\nu+1}}{(\nu+1)!} \mathbf{f}^{(\nu)}([\mathbf{B}_{x,k}], [\mathbf{p}], \mathbf{u}([\tau_k]), [\tau_k]), \quad (5)$$

where a Picard iteration [2, 7] is used to determine the bounding box $[\mathbf{B}_{x,k}]$ with the parameter and control enclosures $[\mathbf{p}]$ and $\mathbf{u}([\tau_k])$, respectively, that are valid for the complete time interval $[\tau_k] := [t_k; t_{k+1}]$.

According to the following four-stage procedure, the simulation approach above for smooth systems of ODEs is generalized to scenarios according to Fig. 4 with transitions between multiple discrete model states. As explained in detail in [1, 16], the required algorithmic steps are given by:

Step 1 Calculation of the bounding box $[\mathbf{B}_{a,k}]$ for the time interval $[\tau_k]$ for the union of all system models S_i which are *active* at $t = t_k$. Here, the term \mathbf{f}_a is a continuously differentiable function enclosing the right-hand sides of *all active* models at $t = t_k$.

Step 2 Check for additionally activated models depending on the states included in the bounding box $[\mathbf{B}_{a,k}]$:

- Repeat **Step 1** if additional models are activated within the time interval $[\tau_k]$ after a modification of \mathbf{f}_a by considering all additionally activated submodels S_i .
- Otherwise, continue with **Step 3**.

Step 3 Interval evaluation of the series expansion in (4), (5) for $\mathbf{f}(\cdot) = \mathbf{f}_a(\cdot)$. For the following identification procedure, it is sufficient to choose $\nu \equiv 1$ due to the fact that measured data are available at dense temporal discretization points.

Step 4 All submodels S_i are deactivated which can no longer be active at $t = t_{k+1}$.

⁴Preconditioning strategies of the state equations for a reduction of the wrapping effect according to, for example, [6, 8] are not considered in this paper, because the consistency test between measured and simulated states during the parameter identification is already sufficient to suppress a blow-up of state enclosures for the application scenario at hand.

4 Verified Parameter Identification

4.1 Fundamental Identification Procedure

For the sake of a verified parameter identification [14, 15], the state enclosures and possible parameter intervals at a point of time $t = t_k$ are stored in a list of L interval boxes

$$\left[\mathbf{z}^{(l)} \right] (t_k) := \left[\begin{array}{c} \left[\mathbf{x}^{(l)} \right] (t_k) \\ \left[\mathbf{p}^{(l)} \right] (t_k) \end{array} \right], \quad l = 1, \dots, L . \quad (6)$$

Out of this list of L boxes, M interval subdivisions are performed, where according to the following criteria, an individual interval l may be selected multiple times under the precondition that it is characterized by a non-zero volume

$$\prod_{j=1}^{n+n_p} \text{diam} \left\{ \left[z_j^{(l)} \right] (t_k) \right\} \neq 0 . \quad (7)$$

Hence, the interval subdivision leads to a new list of intervals of length $L + M - 1$. These interval boxes are propagated until the next measurement point t_{k+1} by means of the verified integration of the IVP described in Sec. 3. The new list of state enclosures at the next measurement point is then given by the boxes $\left[\mathbf{z}^{(l)} \right] (t_{k+1})$, $l = 1, \dots, L + M - 1$.

If selected state variables are measured directly, an intersection of the predicted intervals is performed with the range of uncertain measured data according to $z_1(t_{k+1}) \in [y_m](t_{k+1})$. Here, for sake of a simplified notation, it is assumed that only the first state variable is available as a measured variable. Note that in cases in which a linear or nonlinear combination of several state variables characterizes the measurement, interval Newton techniques or contractor approaches need to be applied to restrict the predicted interval boxes to domains that are consistent with the measured information. For a direct measurement of the first state variable, the before-mentioned intersection yields

$$\left[\tilde{z}_1^{(l)} \right] (t_{k+1}) := \left[z_1^{(l)} \right] (t_{k+1}) \cap [y_m](t_{k+1}) . \quad (8)$$

In the list of $L + M - 1$ interval boxes, all subintervals $\left[z_1^{(l)} \right] (t_{k+1})$ are replaced by $\left[\tilde{z}_1^{(l)} \right] (t_{k+1})$ for which $\left[\tilde{z}_1^{(l)} \right] (t_{k+1}) \neq \emptyset$ holds. All non-overlapping intervals $\left[\tilde{z}_1^{(l)} \right] (t_{k+1}) = \emptyset$ are inconsistent and, therefore, deleted from the list.

In the considered application scenario, the static friction value may change after each standstill of the drive train. Hence, static friction subintervals are replaced with their initial range if standstill is detected for a minimum time span. This information is obtained from the test rig by a corresponding binary signal (start/stop indicator) of the velocity sensor.

After the intersection (8) and the elimination of guaranteed inconsistent intervals, a convex hull of selected boxes with a sufficiently small amount of overestimation can be determined to reduce the number of subintervals to L^* with the new list length $L := L^*$. For that purpose, the merging approach presented in [13] is employed. Note that the replacement of static friction intervals by their initialization values as well as the merging of selected interval boxes can be employed interchangeably.

The block diagram in Fig. 5 gives a summary of the observer-based recursive state and parameter identification procedure.

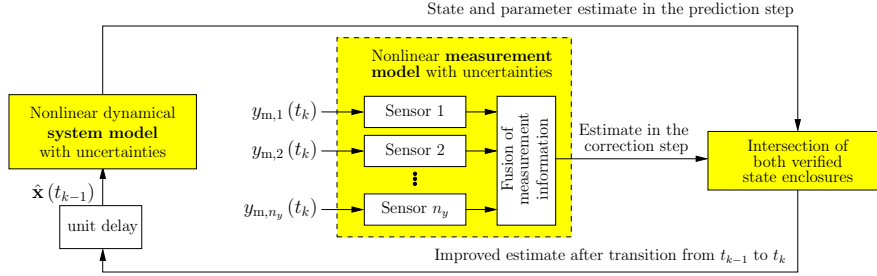


Figure 5: Block diagram of the observer-based identification approach.

4.2 Subdivision Heuristics for the Elimination of Inconsistent Parameter Intervals

In the case of ODE systems with non-smooth right-hand sides, interval uncertainty causes the phenomenon that multiple submodels can be active simultaneously in a verified simulation. Hence, for an efficient experimental parameter identification, both the subdivision procedure and the optimal input parameterization should be set up in such a way that the likelihood for multiple simultaneously active submodels is reduced.

Besides the following subdivision heuristics, this can be done by an appropriate choice of the system input $u(t)$ which enhances the efficiency of the subdivision strategy by a speed-up in the exclusion of inconsistent parameter intervals and, therefore, also ambiguous submodels. Obvious approaches are the choice of slowly increasing input torques for the considered drive train in standstill phases to detect the bounds of the interval for the static friction coefficient accurately. The same also holds for using slow breaking phases before the standstill to again find the bounds for the static friction torque as accurately as possible. In addition, a sensitivity-based input optimization can be used in the sliding friction phase to estimate friction and inertia properties (cf. Sec. 5).

The interval subdivision strategy consists of the following stages⁵. First, the candidate interval (from a temporary list of L' subintervals) to be subdivided is chosen as the one with the largest pseudo volume

$$l^* = \arg \max_{l=1, \dots, L'} \prod_{j=1}^{n+n_p} \text{diam} \left\{ \left[z_j^{(l)} \right] (t_k) \right\}, \quad L' \geq L. \quad (9)$$

Second, ambiguities between static and sliding friction are reduced by splitting the static friction interval if

$$[u](t_k) \cap \text{hull} \left\{ - \left[T_{F,s}^{(l^*)} \right], \left[T_{F,s}^{(l^*)} \right] \right\} \neq \emptyset \quad (10)$$

is satisfied. There, the splitting point for the interval $\left[T_{F,s}^{(l^*)} \right]$ is chosen

- as $\bar{u}(t_k) + \epsilon$, $\epsilon > 0$, if $[u](t_k) > 0$ with $\underline{T}_{F,s}^{(l^*)} < \underline{u}(t_k)$ and $\bar{T}_{F,s}^{(l^*)} > \bar{u}(t_k)$ holds,

⁵In addition to the following heuristics of M interval splittings, it is optional to subdivide also velocity intervals with $\text{diam} \left\{ \left[x_2^{(l^*)} \right] \right\} > \bar{v}$ into each M_v equally large subintervals. Benefits of this extension were demonstrated in [14].

- as $\underline{u}(t_k) - \epsilon$, $\epsilon > 0$, if $[u](t_k) < 0$ with $-\overline{T}_{F,s}^{(l^*)} < \underline{u}(t_k)$ and $-\underline{T}_{F,s}^{(l^*)} > \overline{u}(t_k)$ holds, or
- as the midpoint of $[T_{F,s}^{(l^*)}]$ in all other cases.

Furthermore, to avoid unnecessarily conservative interval bounds in cases where (10) is not true, the following interval bisections are performed (with criteria of higher priority listed first):

- The angular velocity interval⁶ $[x_2^{(l^*)}](t_k)$ is split for

$$\text{diam} \left\{ [x_2^{(l^*)}](t_k) \right\} \geq \text{diam} \left\{ [\beta^{(l^*)}] \right\} , \quad (11)$$

- the interval $[\beta^{(l^*)}]$ is split for

$$\left([\alpha^{(l^*)}] \cdot [x_2^{(l^*)}](t_k) \right) \cap \left([\beta^{(l^*)}] \cdot ([u](t_k) - [T_{F,s}^{(l^*)}]) \right) \neq \emptyset , \quad (12)$$

- else, the interval $[\alpha^{(l^*)}]$ is selected for bisectioning at its midpoint.

The replacement of the static friction interval at standstill of the test rig in Fig. 1 is performed separately for each list element $l = 1, \dots, L$ by the initially assumed range $T_{F,s} \in [T_{F,s}^{\text{ini}}]$ according to

$$\begin{aligned} [T_a^{(l)}] &:= [T_{F,s}^{\text{ini}} ; T_{F,s}^{(l)}] \\ [T_b^{(l)}] &:= [\underline{T}_{F,s}^{(l)} ; \overline{T}_{F,s}^{(l)}] \\ [T_c^{(l)}] &:= [\overline{T}_{F,s}^{(l)} ; \overline{T}_{F,s}^{\text{ini}}] . \end{aligned} \quad (13)$$

This leads to a list of up to the threefold length $3L$, where $[T_{F,s}^{(l)}]$ is replaced by each of the three intervals $[T_a^{(l)}]$, $[T_b^{(l)}]$, and $[T_c^{(l)}]$ which has a non-zero diameter. Also at this point, a subsequent merging of subintervals as mentioned in Sec. 4.1 can be performed (cf. [13]). However, it should be taken into account that merging of intervals is avoided if they originate from different activated discrete model states S_i , $i \in \{1, 2, 3\}$.

5 Sensitivity-Based Input Optimization

Within each piecewise smooth operating regime S_j of the ODE system

$$\dot{\mathbf{x}}(t) = \mathbf{f}_{S_j}(\mathbf{x}(t), \mathbf{u}(t), \boldsymbol{\xi}) , \quad (14)$$

sensitivity equations [11]

$$\dot{\mathbf{s}}_{i,j}(t) = \frac{\partial \mathbf{f}_{S_j}(\mathbf{x}(t), \mathbf{u}(t), \boldsymbol{\xi})}{\partial \mathbf{x}(t)} \cdot \mathbf{s}_{i,j}(t) + \frac{\partial \mathbf{f}_{S_j}(\mathbf{x}(t), \mathbf{u}(t), \boldsymbol{\xi})}{\partial \boldsymbol{\xi}_i} \quad (15)$$

⁶Trisectioning of $[x_2^{(l^*)}](t_k)$ around $x_2 = 0$ is optionally possible, if static and sliding friction may be true simultaneously.

are defined for each parameter ξ_i , $i = 1, \dots, n_\xi$, with the initial conditions $\mathbf{s}_{i,j}(t_0) = \mathbf{0}$. In (15), $\boldsymbol{\xi}$ contains all components of the complete parameter vector \mathbf{p} that need to be identified for the subsystem model S_j .

To determine control signals that lead to a maximization of the sensitivity of the system outputs with respect to the parameters to be identified, the (feedforward) control is either described as a sequence of piecewise constant inputs or by time-dependent polynomials as basis functions with free weighting coefficients. If, for example, Bernstein polynomials

$$\mathbf{b}(t) = [b_{0,M_B}(t) \quad \dots \quad b_{M_B,M_B}(t)]^T \quad (16)$$

of the order M_B with

$$b_{k,M_B}(t) = \binom{M_B}{k} \cdot \left(\frac{t-t_0}{t_1-t_0}\right)^k \cdot \left(\frac{t_1-t}{t_1-t_0}\right)^{M_B-k}, \quad k = 0, \dots, M_B \quad (17)$$

are chosen as the basis functions over a time interval $t \in [t_0; t_1]$, the input vector is defined as

$$\mathbf{u}(t) = \begin{bmatrix} u_{1,0} & \dots & u_{1,M_B} \\ \vdots & & \vdots \\ u_{n_u,0} & \dots & u_{n_u,M_B} \end{bmatrix} \cdot \mathbf{b}(t) . \quad (18)$$

Now, the parameters $u_{l,k}$, $k = 0, \dots, M_B$, are determined for each system input $l = 1, \dots, n_u$ by the minimization of the integral performance criterion⁷ ($\epsilon_i > 0$)

$$J = \int_{t_0}^{t_1} \left((x_1 - x_{1,d})^2 + \sum_{l=1, l \neq i}^{n_\xi} \kappa_l \mathbf{s}_l^T \mathbf{Q}_l \mathbf{s}_l + \frac{1}{\kappa_i \mathbf{s}_{i,j}^T \mathbf{Q}_i \mathbf{s}_{i,j} + \epsilon_i} + \kappa_u \mathbf{u}^T \mathbf{Q}_u \mathbf{u} \right) d\tau . \quad (19)$$

The minimization of the cost function J , defined for the discrete submodel S_j , aims at solving the following tasks simultaneously:

- Tracking of a desired trajectory $x_{1,d}$ for the measured system output x_1 . As before, it is assumed without loss of generality that the system output coincides with the first component of the state vector $\mathbf{x}(t)$.
- The sensitivity of the measured output with respect to the parameter to be identified should be maximized.
- The measured output should be as insensitive as possible with respect to changes in all other parameters.
- A limitation of the control effort can be achieved by including a quadratic penalty term in the cost function.

The weighting factors

$$\mathbf{Q}_i = \mathbf{e}_1 \mathbf{e}_1^T \quad \text{and} \quad \kappa_i = \Delta \xi_i^2 \quad \text{for all} \quad i = 1, \dots, n_\xi \quad (20)$$

are chosen such that tracking errors as well as all sensitivity values are normalized to lie in the same orders of magnitude, when the system input is optimized such that the sensitivity of the output with respect to the parameter ξ_i (indicated by picking out the first entry of $\mathbf{s}_{i,j}$ with the matrix \mathbf{Q}_i) becomes as large as possible. Note that $\Delta \xi_i$ represents the typical range of variations of the i -th parameter to achieve the above-mentioned normalization.

⁷Obviously, also extensions by terminal cost functions at $t = t_1$ are possible.

6 Experimental Results

As a reference solution for the verified parameter identification, the input torque for the electric motor used in [14] is firstly employed. This input leads to the identification results shown in Fig. 6. There, the test rig starts moving at $t \approx 40$ s and performs driving cycles of a length of eight seconds each, starting at standstill, accelerating to a phase with constant velocity, and coming to a standstill again. It can be noticed that both interval parameters $[\alpha]$ and $[\beta]$ can be improved noticeably by the verified identification procedure.

The identification routine was parameterized with $M = 50$ subdivisions at each point at which measured data become available ($t_{k+1} - t_k = 10$ ms) and with additional $M_v = 20$ subdivisions of the velocity interval according to footnote 5. Since the identification routine is evaluated offline for a set of stored measured data, the complete routine has been repeated after the point $t = 80$ s. It can be seen that the improved parameter intervals for $[\alpha]$ and $[\beta]$ lead to enhanced estimates for the static friction torque $T_{F,s}$ in the second and third repetition of the identification, where the final parameter intervals for $[\alpha]$ and $[\beta]$ at the end of the previous run were used for a re-initialization. After each standstill of the test rig, the static friction interval was reset to its initial value according to (13) to account for the phenomenon that the initial breakaway torque is not constant in the application at hand.

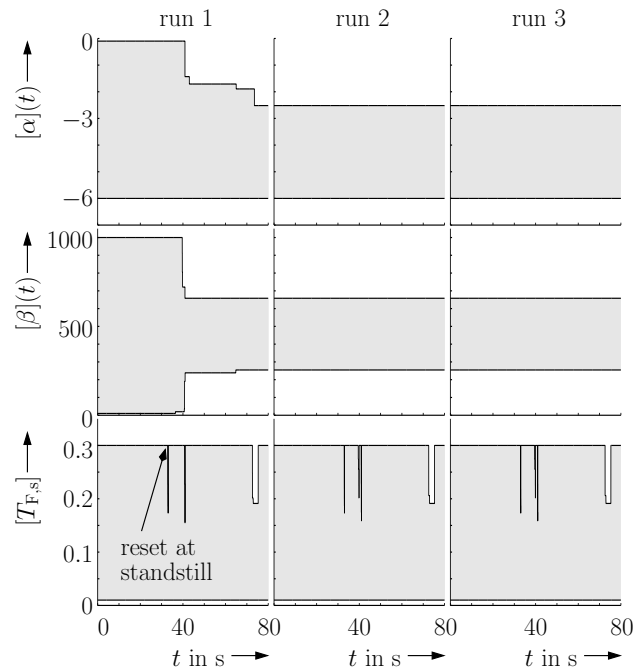


Figure 6: Interval enclosures for the estimated parameters $[\mathbf{p}](t)$ without application of the sensitivity-based input optimization [14].

To enhance the identification quality, the sensitivity-based input optimization routine has been employed. It makes use of the cost function J defined in (19) for the

submodel S_3 (sliding friction with positive velocities). The desired reference trajectory (for a fair comparison to the basic optimization, $t_1 = 8$ s holds) is depicted in Fig. 7a. Switching off all sensitivity terms by weighting factors that are equal to zero, an input torque can be computed according to Fig. 7b by a fifth-order Bernstein polynomial approximation which ensures practically perfect trajectory tracking. This input is adjusted by choosing non-zero weights for the sensitivity terms in (19). The corresponding optimization results are summarized in Fig. 8. According to Fig. 8a, the modified input leads to acceptably small deviations from the reference angle $x_{1,d}(t)$, caused by sharp torque variations at the begin and end of each driving cycle (Fig. 8b).

The modified driving cycle is now employed for the parameter identification with identical numbers of subdivisions as in the reference solution. The estimated interval parameters — that change noticeably as compared to Fig. 6 — are depicted in Fig. 9. It can be seen that the parameter $[\beta]$ is identified significantly sharper during the first execution of the identification routine, where the non-zero input torque was again activated at $t \approx 40$ s. For the second and third run, an intersection with the results of the basic identification was performed since both provide verified parameter estimates. This result highlights that the enhanced actuation of the system typically leads to tighter parameter enclosures with a reduced experimental effort.

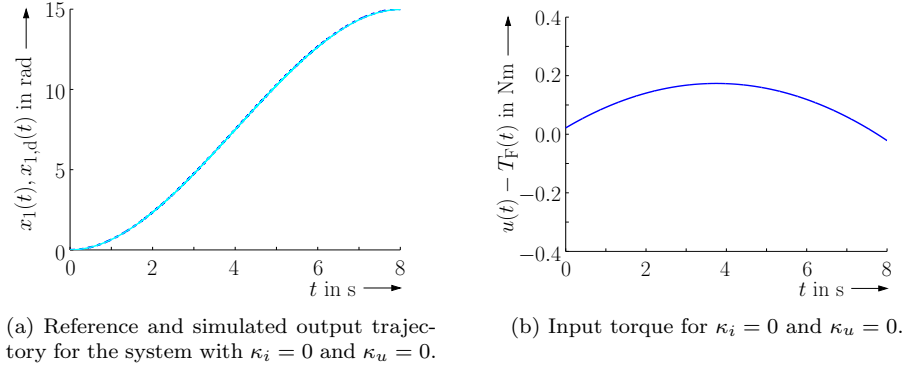


Figure 7: Input optimization (dynamic feedforward control) for a nominal plant model with $\alpha = 4.5$ and $\beta = 65$ without sensitivity extensions of the cost function J .

7 Conclusions and Outlook on Future Work

In this paper, a verified identification procedure was presented for continuous-time dynamic system models with state-dependent transitions between different state-space representations. The challenge for the development of corresponding identification routines is to make sure that ambiguities between the individual subsystem models are reduced as far as possible.

On the one hand, efficient problem-oriented interval subdivision procedures help to rule out submodels that are definitely inconsistent with measured data with bounded tolerances. Here, for example velocity intervals need to be bisected to make sure that the identification routine can distinguish between descriptions for sliding and static friction if mechanical applications are concerned.

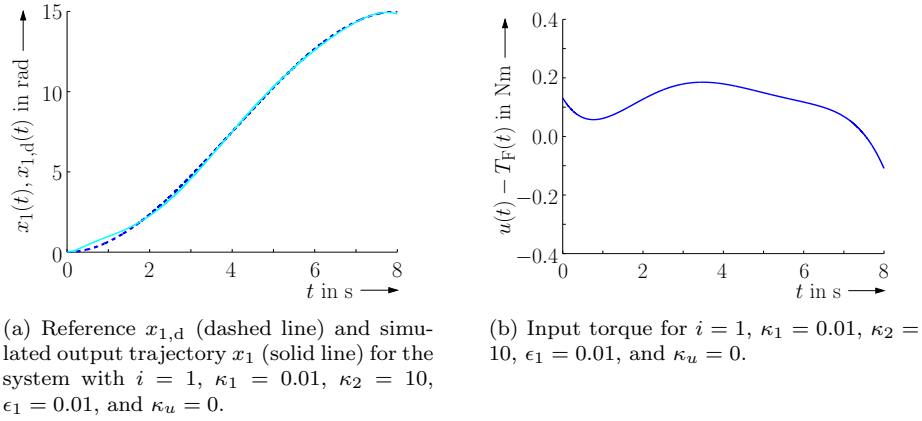


Figure 8: Input optimization (dynamic feedforward control) for a nominal plant model with $\alpha = 4.5$ and $\beta = 65$ with sensitivity extensions of the cost function J ($\xi_1 = \alpha$, $\xi_2 = \beta$).

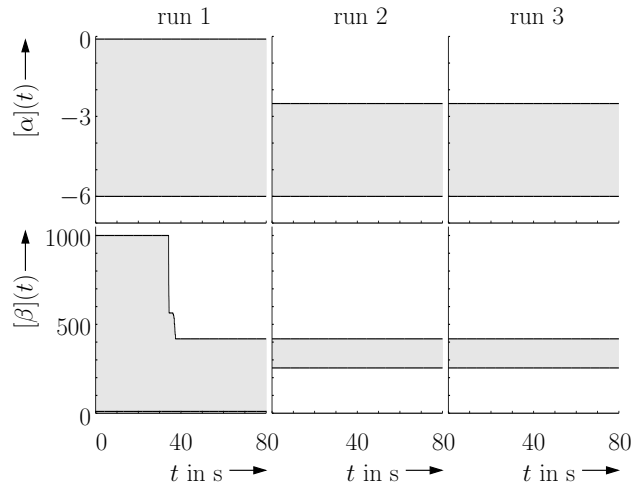


Figure 9: Interval enclosures for the estimated parameters $[p](t)$ with application of the sensitivity-based input optimization.

On the other hand, a novel sensitivity-based procedure was introduced that helps to improve the identifiability of selected parameters by an optimization-based parameterization of the system's control signals.

Future work aims at the validation of the developed optimization procedure for more complex system models, both with a larger number of submodels, more state variables, and higher-dimensional parameter vectors.

References

- [1] E. Auer, S. Kiel, and A. Rauh. A Verified Method for Solving Piecewise Smooth Initial Value Problems. *Intl. Journal of Applied Mathematics and Computer Science AMCS*, 23(4):731–747, 2013.
- [2] Y. Deville, M. Janssen, and P. van Hentenryck. Consistency Techniques for Ordinary Differential Equations. *Constraint*, 7(3–4):289–315, 2002.
- [3] F. Ikhouane and J. Rodellar. *Systems with Hysteresis: Analysis, Identification and Control using the Bouc-Wen Model*. John Wiley & Sons, Inc., New Jersey, 2007.
- [4] L. Jaulin, M. Kieffer, O. Didrit, and É. Walter. *Applied Interval Analysis*. Springer–Verlag, London, 2001.
- [5] R. Krawczyk. Newton-Algorithmen zur Bestimmung von Nullstellen mit Fehler-schranken. *Computing*, 4:189–201, 1969. In German.
- [6] R. Lohner. Enclosing the Solutions of Ordinary Initial and Boundary Value Problems. In E. W. Kaucher, U. W. Kulisch, and C. Ullrich, editors, *Computer Arithmetic: Scientific Computation and Programming Languages*, pages 255–286, Stuttgart, 1987. Wiley-Teubner Series in Computer Science.
- [7] N. S. Nedialkov. *Computing Rigorous Bounds on the Solution of an Initial Value Problem for an Ordinary Differential Equation*. PhD thesis, Graduate Department of Computer Science, University of Toronto, 1999.
- [8] N. S. Nedialkov. Interval Tools for ODEs and DAEs. In *CD-Proc. of 12th GAMM-IMACS Intl. Symposium on Scientific Computing, Computer Arithmetic, and Validated Numerics SCAN 2006*, Duisburg, Germany, 2007. IEEE Computer Society.
- [9] N. S. Nedialkov and M. v. Mohrenschildt. Rigorous Simulation of Hybrid Dynamic Systems with Symbolic and Interval Methods. In *Proc. of the American Control Conference ACC*, pages 140–147, Anchorage, USA, 2002.
- [10] A. Neumaier. *Interval Methods for Systems of Equations*. Cambridge University Press, Encyclopedia of Mathematics, Cambridge, 1990.
- [11] A. Rauh, J. Kersten, E. Auer, and H. Aschemann. Sensitivity-Based Feedforward and Feedback Control for Uncertain Systems. *Computing*, (2–4):357–367, 2012.
- [12] A. Rauh, M. Kletting, H. Aschemann, and E. P. Hofer. Interval Methods for Simulation of Dynamical Systems with State-Dependent Switching Characteristics. In *Proc. of the IEEE Intl. Conference on Control Applications CCA 2006*, pages 2243–2248, Munich, Germany, 2006.

- [13] A. Rauh, M. Kletting, H. Aschemann, and E. P. Hofer. Reduction of Overestimation in Interval Arithmetic Simulation of Biological Wastewater Treatment Processes. *Journal of Computational and Applied Mathematics*, 199(2):207–212, 2007.
- [14] A. Rauh, L. Senkel, and H. Aschemann. Experimental Comparison of Interval-Based Parameter Identification Procedures for Uncertain ODEs with Non-Smooth Right-Hand Sides. In *CD-Proc. of IEEE Intl. Conference on Methods and Models in Automation and Robotics MMAR 2015*, Miedzyzdroje, Poland, 2015.
- [15] A. Rauh, L. Senkel, and H. Aschemann. Verified Parameter Identification for Dynamic Systems with Non-Smooth Right-Hand Sides. In *Proc. of the 16th GAMM-IMACS International Symposium on Scientific Computing, Computer Arithmetic, and Validated Numerics SCAN 2014*, volume 9553 of *Lecture Notes in Computer Science*, pages 236–246, Würzburg, Germany, 2016.
- [16] A. Rauh, Ch. Siebert, and H. Aschemann. Verified Simulation and Optimization of Dynamic Systems with Friction and Hysteresis. In *Proceedings of ENOC 2011*, Rome, Italy, 2011.
- [17] R. Rihm. Enclosing Solutions with Switching Points in Ordinary Differential Equations. In *Computer Arithmetic and Enclosure Methods. Proceedings of SCAN 91*, pages 419–425. Amsterdam: North-Holland, 1992.
- [18] R. Rihm. *Über Einschließungsverfahren für gewöhnliche Anfangswertprobleme und ihre Anwendung auf Differentialgleichungen mit unstetiger rechter Seite*. PhD thesis, Universität Karlsruhe, 1993. In German.